Study on drag coefficient via dielectric barrier discharge (DBD) plasma actuators

M. Bigdeli, R. Mohammadi, J. Bigdeli, V. Monfared*
Department of Mechanical Engineering, Zanjan Branch, Islamic Azad University, Zanjan, Iran

Nowadays, due to the wide application and importance of active control methods such as Dielectric Barrier Discharge (DBD) plasma actuators, they are used in industries such as aerospace, propellers, and wind turbines to reduce the flow separation region and vortices around these objects (important applications). Accordingly, theories that can improve the efficiency in the aviation industry have drawn much attention. The larger the flow separation region around the airfoil, the more the vortices and return flows, and the larger the drag force. This leads to undesirable dissipation, especially in fuel, and instability of the aircraft (importance of the research work). The drag coefficient has a significant effect on the performance of the airplane, especially at high velocities. Hence, a method that can control the air flow on the airfoil and decrease the drag coefficient and the associated dissipation will be helpful. In this research, the airflow over a NACA0012 airfoil has been designed and analyzed in ANSYS Fluent software. In this method, two-dimensional airfoil aerodynamics is considered, and the high-Re airflow around the airfoil is analyzed. Moreover, the UDF code of the plasma is defined as a body force at an optimal and sensitive location of the airfoil (flow separation region). Subsequently, the drag coefficient is evaluated at a constant Re and different angles of attack. As a result, the drag coefficient at different angles of attack is smaller for when plasma is defined on the airfoil (plasma-on) compared to when plasma is inactive (plasma-off). Furthermore, it is shown that the pressure distribution around the airfoil is improved using plasma actuators.

(Received January 26, 2021; Accepted May 11, 2021)

Keywords: Plasma (Dielectric barrier discharge), Drag coefficient, Body force, Pressure distribution

1. Introduction

The characteristics of the aerodynamic force have significance in engineering and scientific applications such as aircraft, ships, helicopters, compressors, turbines, fans, pumps, wind tunnels, hydraulic canals, mills, and numerous other industries [1]. However, the most important application of aerodynamics is in aerospace and automotive engineering. Nowadays, aerodynamics has gained importance in the aviation industry, and engineers attempt to design aircraft wings such that the least air resistance and smallest flow separation region are obtained. The drag coefficient is used to indicate the aerodynamic state and can affect other factors such as maximum velocity, stability, fuel consumption, etc. A critical angle in an aircraft is a situation when the flow separation region behind the airfoil increases with an increase in the angle of attack, resulting in a sudden decrease in the lift coefficient and a strong increase in the drag coefficient. This eventually leads to a stall of the aerodynamic section and is generally undesirable because it causes energy dissipation and a reduction in aircraft efficiency [2, 3].

Given the wide application of the phenomenon of flow around rigid objects, the study of momentum transfer has always drawn the attention of researchers. Theories that can somehow improve the efficiency of surfaces facing the fluid flow are of considerable interest. Aspects such as computing the aerodynamic forces and pressure distribution, investigating vortex separation and mechanisms governing the formation of vortices and the growth downstream of the flow are known as challenging problems in this field. Nowadays, the use of plasma actuators has attracted attention due to the possibility of creating a body force and, therefore, controlling the airflow

* Corresponding author: vahid_monfared@alum.sharif.edu

around rigid objects. These actuators are among the most proposed methods in flow control due to their availability, lack of need for special repairs, a very short response time, and low energy consumption [4].

This research aims to examine the drag coefficient and pressure distribution around the NACA0012 airfoil using plasma (DBD) actuators. Among research works conducted in this area, one can mention the research by Corke et al. [5] who used weakly-ionized plasma actuators to increase the lift in the NACA0009 airfoil. They observed that the use of these actuators led to a simultaneous increase in the lift and drag forces, which was considered a flaw. Subsequently, they observed that the use of several actuators can eliminate the increase in the drag force [5]. Benard et al. [6] addressed the control of the lift and drag forces in the flow around a NACA0015 airfoil using an AC plasma actuator and demonstrated that the application of an electric field can simultaneously improve the lift force and reduce the drag force [6]. Morshed et al. [7] studied drag in 4 different profiles in a wind tunnel. After performing experiments, they discovered that created drag considerably depends on the shape. They also analyzed drag in 4 profiles, including sphere, cylinder, symmetrical airfoil (NACA 0015), and cambered airfoil (NACA 4415). These profiles were tested in the wind tunnel at velocities of 10, 15, 20, 25, and 30 meters per second. The authors concluded from their experiments that the drag created in the cambered airfoil (NACA 4415) is smaller than those in the other profiles and that the largest drag corresponded to the spherical profile [7]. Roy et al. [8] studied the drag coefficient on a vehicle using serpentine dielectric barrier discharge actuators. They concluded that a similar linear plasma actuator cannot reduce the drag at the studied speeds. Furthermore, they claimed that the empirical data obtained for linear and serpentine plasma actuators under quiescent operating conditions indicate the strong effect of the serpentine design on the near-wall flow structure and the resulting drag; according to their results, for a specific actuator arrangement, the measured drag dropped by more than 14% and 10% at speeds of 26.8 m and 31.3 m, respectively, indicating an opportunity to save energy in full-scale ground vehicles [8]. Also, the considerable and applied research works have been done and analyzed about analysis of the drag force and coefficients [12-16], and the airfoil/composite [17-21] airfoils in the recent years. For example, a comparison study has been theoretically done to analyze the supersonic flow over conical bodies of three cross sections of elliptic, circular, and squircle shapes utilizing the method of Perturbation to get the flow variables [13].

In this research work, it has been used DBD actuators and the Spallart-Almaras turbulence model to study the drag coefficient and pressure distribution at high Re and to demonstrate the reduction in the drag coefficient in various angles of attack.

2. The governing equations and methodology

This study attempts to study the flow around the airfoil, NACA 0012 airfoil geometry, modeling and meshing of the geometry, and the effects related to plasma actuators. For this purpose, an airfoil is considered in the flow regime and its momentum, continuity and turbulence equations are solved numerically.

2.1. NACA Airfoil Geometry 0012

Here, the intended airfoil is the standard NACA0012 airfoil as one of the 4-digit NACA airfoils. The reason for choosing this airfoil is its wide range of applications including general aviation, supersonic jets, helicopter blades, ship bow, rocket fins, and many more. This airfoil has been used as the wing section in some aircraft, including the Cessna 152. Also, due to its symmetrical geometry, the manufacturing process is simple and does not require complex equipment. Moreover, because of being wider compared to other airfoils (with a width-to-chord ratio of 24%), it is easier to install electrodes and remove pressure measurement tubes from airfoil damping tests [2, 9]. A schematic of this airfoil and its relative coordinates is shown in Fig. 1 [10].

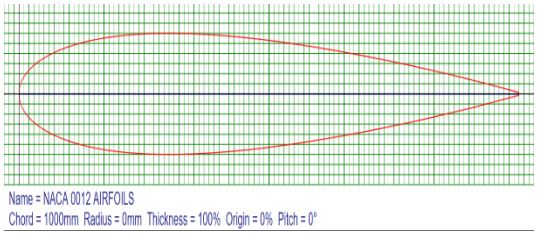

Fig. 1. Modeled NACA 0012 airfoil coordinates view [10]

2.2. Modeling and meshing

The goal here is to examine the flow near an airfoil. To this end, the computational domain must first be drawn. Then, the domain must be meshed, and the boundary conditions must be specified. Finally, the results must be derived after solving the equations numerically.

2.2.1 Computation space and meshing

Fig. 2 presents a computational domain along with meshing that includes boundary conditions, namely flow inlet, flow outlet, and airfoil wall. As can be seen, a finer mesh is used near the airfoil, as the computational accuracy in these areas should be greater.

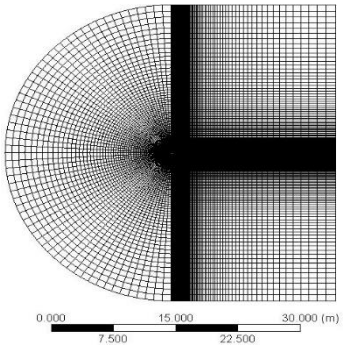

Fig. 2. NACA 0012 airfoil meshing.

2.2.2. Boundary conditions

In this study, a Reynolds number of 1.4×10^6 is assumed for the flow around the airfoil, as can be calculated from Eq. (1) [8].

$$Re = \frac{\rho v c}{\mu} \tag{1}$$

where "ρ" is density, "v" is velocity of the flow, "C" is the chord length of the airfoil, and "μ" is the dynamic viscosity of the air. Also, the problem definition and flow simulation method using Ansys Fluent software is as follows [8]. The reference parameters in this research are as in Table 1.

Table 1. Reference parameters.

Parameter	**Value**	**Symbol**	**Unit**
Reynolds number	-	*Re*	-
Density	1.225	ρ	kg/m^3
dynamic viscosity	1.7894×10^{-5}	μ	$kg/m.s$
Airfoil chord length	1	*C*	*m*
Flow velocity	20	*V*	*m/s*

Table 2 shows the equations in the numerical solution. As shown in the table, four equations are needed to model fluid motion and heat transfer in a porous medium. The first is the continuity equation, which states that no mass of fluid is created or destroyed. In addition, two momentum equations are required, one in the direction of the flow and the other normal to this direction. Finally, one turbulence equation is used because the modeling in this study is based on a one equation model.

Table 2. Number of equations needed for modeling.

Number	Equations
1	Continuity
2	Navier-Stokes
1	Turbulence

What is stated here is for solving the flow field, meaning that plasma is inactive. With the addition of plasma as a body force written in C programming language using Visual Studio programming software, it is defined by compiling in Ansys Fluent software.

3. Results and discussion

This section studies the pressure distribution and the drag coefficient when the plasma is defined as a body force on the airfoil and evaluates and compares the results to those of the normal mode (plasma-off), including the following:

1- Examining the pressure contours around the NACA 0012 airfoil in plasma-on and plasma-off modes.

2- Examining and computing the drag coefficients in terms of the angles of attacks of 5°, 10°, 12°, 14°, 15°, 16°, 17°, 18°, and 19° in plasma-off and plasma-on modes.

3.1. Investigating the pressure contour

In this section, the static pressure contour in the plasma-on and plasma-off modes are examined to know which areas of the airfoil experience the largest and smallest pressures in each mode. For this purpose, the analysis obtained at the angle of attack of 15°, as a large and near-critical angle of attack, is used for comparison.

3.1.1. Pressure contour in the plasma-off mode

Fig. 3 displays the static pressure contour at a flow angle of 15°. As shown in the figure, the highest pressure is at the leading edge, and the smallest pressures are observed at the top of the airfoil; thus, the airfoil prevents the motion of the fluid.

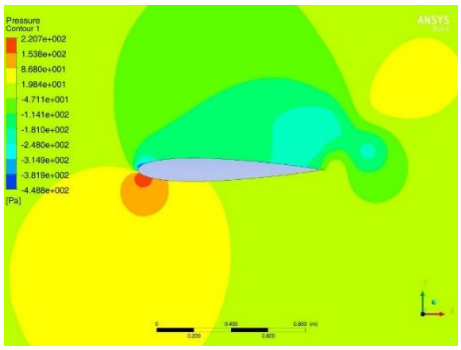

Fig. 3. Static pressure contour at an angle of attack of 15° *(plasma-off).*

3.1.2. Pressure contour in the plasma-on mode

Fig. 4 displays the static pressure contour at a flow angle of 15° in the plasma-on mode. Just as the largest static pressure in the plasma-off mode was exerted at the leading edge of the airfoil, after defining the plasma and activating it as a body force on the airfoil, the static pressure at the bottom of the airfoil is increased (high-pressure region), and the static pressure is reduced at the top of the airfoil (low-pressure region). As seen in the figure, the pressure distribution at the bottom of the airfoil is considerably higher, leading to an increase in the lift force.

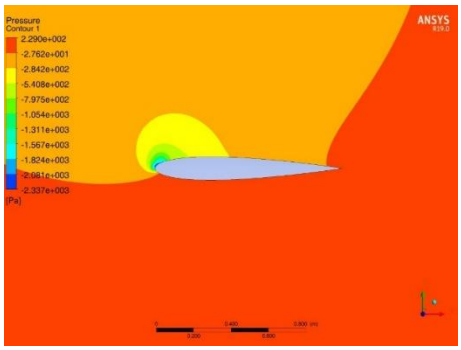

Fig. 4. Static pressure contour at an angle of attack of 15° *(plasma-on).*

3.2. Investigating the drag coefficient

As shown in Fig. 5, the drag coefficient results when the plasma is off has been computed at angles of attack of 5°, 10°, 12°, 14°, 15°, 16°, 17°, 18°, and 19°. The results show that with an increase in the angle of attack, the drag coefficient also increases, and the largest increase in the drag coefficient is observed at the angles of attacks larger than 15°. For comparison and validation, the drag coefficient experimental results by Eftekhari et al. [11] have been used. Fig. 5 shows that the drag coefficients obtained in the present study are close to the experimental ones by Eftekhari et al. at identical angles of attack.

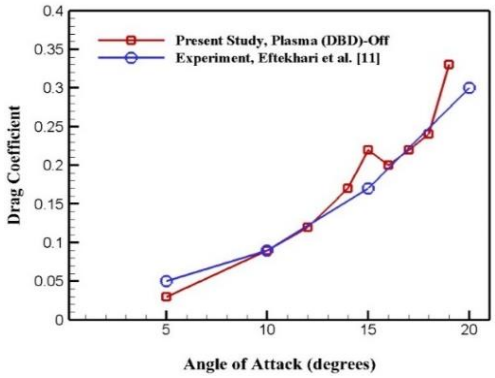

Fig. 5. Drag coefficient results in the plasma-off mode versus angle of attack and a comparison with the experimental data by Eftekhari et al. [11].

As shown in Figs. 6. (a), (b), in the plasma-on mode, the drag coefficients at angles of attack similar to those for the plasma-off mode have decreased. The obtained results show that the dielectric barrier discharge actuators have a positive effect on the aircraft wing and reduce the drag force considerably.

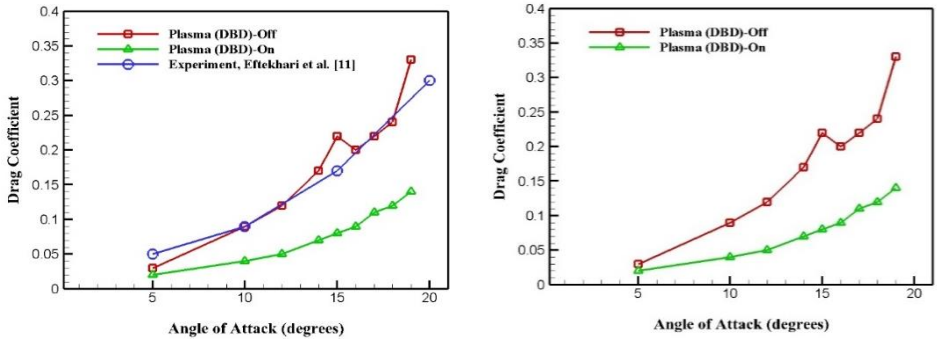

(a) *(b)*

Figs. 6. (a) Results of drag coefficients versus angle of attack in plasma-off and plasma-on modes, (b) Results of drag coefficients in plasma-on and plasma-off modes compared to the experimental results by Eftekhari et al. [11].

4. Conclusions

In this research, the drag coefficient results in the plasma-off mode were compared to the experimental results by Eftekhari et al. [11]; then, the effect of dielectric barrier discharge actuators on the NACA 0012 airfoil was examined to reduce the drag coefficient. The general results are as follows:

- The drag coefficient results in the plasma-off mode were close to the experimental results by Eftekhari et al. [11] at identical angles of attack.
- The use of dielectric barrier discharge actuators at an optimal position on the NACA 0012 airfoil reduces the drag coefficients at various angles, leading to less energy loss.
- Fig. 6 indicates that in the plasma-off mode, the drag coefficients strongly increase from the angle of attack 15°upward, which are critical and super-critical angles of attack. This is generally undesirable, and by the addition of plasma as a body force, the drag coefficients of these critical angles decreased.
- The largest static pressure in the plasma-off mode was observed at the leading edge of the airfoil, and the smallest static pressure in this mode was observed at the top of the airfoil; hence, the airfoil prevents the motion of the fluid.
- After the activation of plasma (DBD) actuators, the pressure distribution at the bottom of the airfoil was considerably higher, leading to an increase in the lift force.
- Plasma (DBD) actuators have a positive effect on the aircraft wing and the aerodynamic forces, finally resulting in improved aircraft efficiency.
- It is recommended to install 2 or 3 dielectric barrier discharge actuators on different parts of the airfoil to control the flow and pressure on the airfoil.

References

[1] M. H. Masud, Naim-Ul-Hasan, Amit Md. Estiaque Arefin, Mohammad U. H. Joardder, AIP Conference Proceedings, December 2016.
[2] John D. Anderson Jr, Fundamentals of Aerodynamics, Fifth Edition, McGraw-Hill series in aeronautical and aerospace engineering.
[3] John S. Duncan, Pilot's Handbook of Aeronautical Knowledge, U.S. Department of Transportation Federal Aviation Administration Flight Standards Service, 25 (2016).
[4] S. Pal, R. Sriram, M. V. Srisha Rao, G. Jagadeesh, 28th International Symposium on Shock Waves, (2012), Springer, Berlin, Heidelberg.

[5] T. Corke, E. Jumper, M. Post, D. Orlov, T. McLaughlin, Application of Weakly-Ionized Plasmas as Wing Flow-Control Devices, AIAA Paper 2002-0350, 40th AIAA Aerospace Sciences Meeting and Exhibit, Reno, NV, U.S.A.
[6] N. Benard, J. Jolibois, E. Moreau, Journal of Electrostatics, 133 (2009).
[7] Munzarin Morshed, Shehab Bin Sayeed, Syed Abdullah Al Mamun and GM Jahangir Alam, Journal of Modern Science and Technology **2**(2), 113 (2014).
[8] Subrata Roy, Pengfei Zhao, Arnob DasGupta, Jignesh Soni, Aip Advances **6**, 025322 (2016).
[9] R. H. Barnard, D. R. Philpott, Aircraft Flight, A description of the physical principles of aircraft flight, Fourth Edition.
[10] www.airfoiltools.com
[11] Shahrooz Eftekhari, Abdulkareem Shafiq Mahdi Al-Obaidi, Journal of Aerospace Technology and Management **11**, (2019).
[12] U. Yusupaliev, Plasma Physics Reports volume **31**, 497 (2005).
[13] A. Baradaran Rahimi, International Journal of Engineering **25**(3), 231 (2012) .
[14] Lu Wang, Zhi-Ying Zheng, Jia-Qi Bao, Tong-Zhou Wei, Wei-Hua Cai, Feng-Chen Li, Canadian Journal of Physics **95**(11), 1115 (2017).
[15] J. Busch, W. Barthlott, M. Brede, W. Terlau, Phil. Trans. R. Soc. A **377**, 20180263 (2019).
[16] Kumar Amit, Kumar Navin, Das Rakesh, Lakhani Piyush, Bhushan Bharat, Phil. Trans. R. Soc. A **377**, 20190132 (2019).
[17] Vahid Monfared, A displacement based model to determine the steady state creep strain rate of short fiber composites, Composites Science and Technology 2015, 107, 18-28.
[18] Vahid Monfared, A micromechanical creep model for stress analysis of non-reinforced regions of short fiber composites using imaginary fiber technique, Mechanics of Materials 2015, 86, 44-54.
[19] Sunil K. Sinha, Richard P. Zylka, Vibration analysis of composite airfoil blade using orthotropic thin shell bending theory, International Journal of Mechanical Sciences, Volume 121, February 2017, Pages 90-105.
[20] Vahid Monfared, Chapter 31 - Problems in short-fiber composites and analysis of chopped fiber-reinforced materials, New Materials in Civil Engineering, 2020, Pages 919-1043
[21] Mohammad Bigdeli, Vahid Monfared, Investigation and Comparison of Stall Angle of Airfoil NACA 0012 in Reynolds Number of 3×10^6 with K − ω SST, Realizable k-ε, Spalart-Allmaras Turbulence Models, Comptes Rendus de l 'Academie Bulgare des Sciences, Proceedings of the Bulgarian Academy of Sciences, 2020, 73 (3), 394-402.